Assessment of Photoreceptor Impairment in Macular Degeneration

Ph.D. Program in the Integrative Oriental and Western

Medical Sciences

Graduate School of Medicine and Pharmaceutical Sciences

University of Toyama

Tomoko Ueda Consolvo

Abstract

Purpose

To evaluate the early changes of photoreceptor structure in macular degeneration and the association between photoreceptor density and visual function. We also investigated ways to prevent photoreceptor loss in macular degeneration.

Methods

The following four studies were conducted. Study 1: Six patients with retinitis pigmentosa were studied retrospectively. The changes of cone density on adaptive optics (AO) fundus camera, visual acuity and visual field were assessed over two years. The correlations between cone density and visual function were evaluated. Study 2: This was a prospective observational single-center study. We investigated the changes of cone density of 29 patients who had been treated with hydroxychloroquine (HCQ) for the first time and followed with AO fundus camera for a minimum of two years. The changes of visual acuity and foveal thickness were also analyzed. Study 3: 64 consecutive patients with neovascular age-related macular degeneration (nAMD) were evaluated for endothelial function by use of peripheral arterial tonometry (EndoPAT 2000; Itamar Medical, Caesarea, Israel). We tallied the number of anti-VEGF treatments over two years and determined the correlation between the number of anti-VEGF injections and endothelial function expressed as the reactive hyperemia index (RHI). Study 4: This was a retrospective, observational case study of eleven eyes in eleven patients with myopic choroidal neovascularization (mCNV) followed with optical coherence tomography angiography (OCTA) for a minimum of three years. The relationship between the changes of mCNV size and recurrences treated with anti-vascular endothelial growth factor (VEGF) agents was analyzed. We also assessed the relationship between the changes of mCNV size and the size of chorioretinal atrophy (CRA) which causes severe visual impairment due to the loss of photoreceptor.

Results

Study 1: AO fundus camera detected a decrease of cone density over 2 years in all RP patients. Five of six RP patients, however, did not show remarkable changes in visual acuity, foveal sensitivity, and photoreceptor thickness. The decrease of photoreceptor density started prior to the progression of visual impairment. Study 2: AO showed no change in cone density in first two years of HCQ use. VA and foveal thickness did not show obvious change, either. Study 3: The lnRHI correlated with the number of anti-

VEGF injections (r = -0.56; P = 0.030). The multiple regression analysis revealed that endothelial function, neovascular subtypes, and treatment regimens were associated with the number of injections. Study 4: Without recurrences, the size of CNV did not show remarkable changes in three years. Without prompt treatment, however, the size of CNV increased significantly. There was a correlation between mCNV enlargement and CRA size at 3 years (Spearman correlation coefficients, r = 0.846; p=0.002; n=11).

Conclusions

In macular degeneration, the onset of photoreceptor decrease occurs prior to visual impairment. AO fundus camera may give us valuable information to monitor and predict the progression of macular degeneration. To prevent photoreceptor loss in macular degeneration secondary to CNV, improving endothelial function may be an effective approach by suppressing the recurrence of CNV. And once the CNV reoccur, prompt treatment is critical to prevent enlargement of CNV which might cause severe visual impairment due to the photoreceptor loss during CRA development.

Introduction

The macula is the center of all human vision and is critically unique to our visual function. Cone photoreceptors are localized in the macula and responsible for high-resolution and color vision. Macular degeneration causes severe central vision loss due to progressive degeneration of photoreceptors. Losing central vision makes it difficult to see faces, read, or drive and causes significant stress on patients.

To examine loss of cone photoreceptors in macular degeneration, we performed direct observation of cone photoreceptors using adaptive optics (AO) fundus camera. An AO system consists of a wavefront sensor that measures aberrations of the whole eye and a deformable mirror or a spatial light modulator that compensates for these aberrations in living eyes [1-5]. AO fundus camera allows researchers to obtain clear images of individual cone photoreceptors in patients with various retinal diseases [6,7]. We examined cone structure using AO fundus camera in patients with macular degeneration caused by retinitis pigmentosa or hydroxychloroquine retinopathy (HCQR). We evaluated the early changes of photoreceptor structure in macular degeneration and the association between photoreceptor density and visual function.

Macular degeneration also occurs secondary to choroidal neovascularization (CNV) in age-related macular degeneration (AMD) and myopic choroidal neovascularization (mCNV). Although they are the leading cause of irreversible visual impairment among adults worldwide, the ways to prevent photoreceptors loss are still unexplored. We investigated an improvable factor; endothelial function, which might be related to CNV recurrence and CNV response to treatments. We also examined the effects of CNV reactivation on the changes of the CNV size and the correlation between CNV size and chorioretinal atrophy (CRA) which causes photoreceptors loss.

Our four studies in this research are reported in following published papers.

(1) The association between cone density and visual function in the macula of patients with retinitis pigmentosa. Graefes Arch Clin Exp Ophthalmol. 2019 (Study 1)
(2) Hydroxychloroquine's Early Impact on Cone Density. J Ophthalmol. 2021 (Study 2)
(3) The relationship between vascular endothelial dysfunction and treatment frequency in neovascular age-related macular degeneration. Jpn J Ophthalmol. 2017 (Study 3)
(4) Using optical coherence tomography angiography to guide myopic choroidal

neovascularization treatment: a three-year follow-up study. Graefes Arch Clin
Exp Ophthalmol. 2021 (Study 4)

Methods

The study was approved by the Institutional Review Board of the University of Toyama,
and the procedures used conformed to the tenets of the Declaration of Helsinki. After the
nature and possible consequences of the study were explained to the patients, written
informed consent was obtained from each.

(1) The association between cone density and visual function in patients with retinitis pigmentosa. (Study 1)

Patient selection

We enrolled 6 patients with RP who visited Toyama University Hospital between March
2013 and May 2017 and examined all 12 eyes of these patients. The inclusion criteria
were (1) a diagnosis of RP by fundus appearances and reduced amplitudes of
electroretinograms; (2) aminimum follow-up of 2 years; (3) no advanced cataract, corneal
opacity, or vitreous hemorrhage which could interfere with the use of AO fundus imaging.
The exclusion criteria were (1) other retinal diseases such as cone-rod dystrophy, cone
dystrophy, retinal inflammatory diseases, autoimmune paraneoplastic retinopathy, or
drug toxicity, and (2) patients with poor image quality.

All patients underwent comprehensive ophthalmic examinations including
measurement of best-corrected decimal visual acuity, measurement of intraocular
pressure, and examination by slit-lamp biomicroscopy, OCT (RS-3000 Advance; Nidek,
Aichi, Japan), Humphrey Field Analyzer (HFA; Carl ZeissMeditec,Dublin, CA) with the
10–2 Swedish Interactive Threshold Algorithm (SITA) standard program, and rtx 1™
AO fundus camera (Imagine Eyes, Orsay, France).

Analysis of adaptive optics images

AO images were taken in the nasal, temporal, superior, and inferior areas at 0.5 mm
from the foveal center in each eye. The images were processed with software tools
supplied by the manufacturer (CK V.1.3 and AO Detect V.0.1). These images were

registered using a cross-correlation method and averaged to produce a final image with an enhanced signal-to-noise ratio. Montage images were created using image editing software (Photoshop Elements 11; Adobe, Mountain View, CA). Cone counting was performed in 3 areas in each of 4 directions (nasal, temporal, superior, and inferior) at 0.5 mm from the foveal center. In each direction, 3 different counting areas were picked up at 0.5 mm from the foveal center. The size of the counting area was chosen to avoid retinal capillaries and set as 100 µm× 100 µm square. The same measured area was ensured by the location and the shape of retinal capillaries. Scales of the macular images were measured using Littmann's method. Cone density was calculated automatically using AO Detect software (Imagine Eyes). We obtained the mean density from the densities in 3 areas. Changes in the mean cone density at the same locations in each eye were followed-up at the baseline, and 6, 12, 18, and 24 months after the baseline.

Retinal thickness measurements

We used OCT to obtain horizontal B-scan images through the fovea of each eye.We measured the total foveal thickness (the distance between the vitreoretinal interface and the inner border of the RPE), the thickness of the outer nuclear layer (ONL; the distance between the outer plexiform layer and external limiting membrane (ELM)), and the thickness of the inner segment (IS) + outer segment (OS) (the distance between the ELM and the inner border of the RPE) at the center of the fovea (Figure 1).
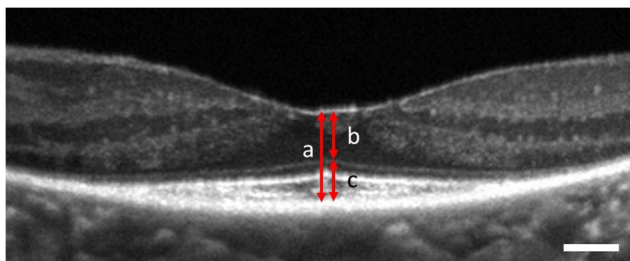

Figure 1 Measurements included the total foveal thickness, the left directional arrow (a), the thickness of the outer nuclear layer, the distance between the outer plexiform layer and external limiting membrane (ELM), superior of the right directional arrow (b), and the thickness of the inner segment +outer segment (the distance between the ELM and the inner border of the RPE), inferior of the right directional arrow (c). Scale bar = 100 µm

Evaluation of foveal sensitivity

A HFA with the 10–2 SITA standard program was used to evaluate foveal sensitivity. The

sensitivity is expressed in a logarithmic scale of decibels (dB), where a higher dB value corresponds to better visual sensitivity. We calculated the mean sensitivity from dB of the 4 points at a 2° × 2° area centered at the fovea in each HFA result. Statistical analysis All statistical analyses were carried out using JMP statistical discovery software (version 11; SAS Institute, Cary, NC). The paired t test was performed for comparison of two groups and one-way ANOVA followed by post hoc test for comparison of multiple groups. Statistical significance was defined as $p < 0.05$.

(2) Hydroxychloroquine's Early Impact on Cone Density. (Study 2)

Patient selection

We carried out a two-year prospective observational study from November 2015 to October 2018 at a single center (Toyama University Hospital, Japan) in 29 eyes of 29 patients (1 men, 28 women) who were introduced HCQ for the first time. Inclusion criteria were 1) patients with no history of taking HCQ, and 2) no advanced cataract, corneal opacity, or vitreous hemorrhage which could interfere with the use of AO fundus imaging. If quality of AO images were same in both eyes, the right eye was selected. The exclusion criteria were 1) other retinal diseases such as cone-rod dystrophy, cone dystrophy, retinal inflammatory diseases, autoimmune paraneoplastic retinopathy, or drug toxicity, and 2) patients with poor image quality. In total AO fundus images were taken in 33 patients and 4 patients were excluded because of the poor quality.

All patients underwent comprehensive ophthalmic examinations including measurement of best-corrected visual acuity, measurement of intraocular pressure, and examination by slit-lamp biomicroscopy, OCT (RS-3000 Advance; NIDEK Co, Ltd, Aichi, Japan), Humphrey Field Analyzer (HFA; Carl Zeiss Meditec, Dublin, CA) with the 10–2 Swedish Interactive Threshold Algorithm (SITA) standard program, and rtx 1™ AO fundus camera (Imagine Eyes, Orsay, France).

Analysis of adaptive optics images

For each eye, a high-resolution image of the foveal center and 4 more images of the area (nasal, temporal, superior, and inferior) around it were captured by moving the fixation point. The i2k retina software (Dual Align TM LLC, Clifton Park, NY) was used to obtain image alignment and multi-image mosaics. After image processing, we had pictures of an 6° × 6° area of the retina with fovea in the center. Measurements of cone density were performed automatically using the AO detect-mosaic V2.0b17(Imagine Eyes, orsay,

France). The axial length (AL) of the eye was required to measure cone density. AL was measured with the OA-2000 (Tomey, Nagoya, Japan) optical axial length biometer. Cone counting was performed in each of 4 quadrants (nasal, temporal, superior, and inferior) at 0.75mm from the foveal center. The size of the counting area was chosen to avoid retinal capillaries and set as 50μm×50μm square (software default size). The same measured area was ensured by the location and the shape of retinal capillaries. Changes in the mean cone density at the same locations in each eye were followed-up at the baseline, and 6, 12, 18, and 24 months after the baseline.

Foveal thickness measurement

Foveal thickness was manually segmented and defined as distance from the vitreoretinal interface to the inner border of the RPE. The observer measured the foveal thickness using the caliper function built into the linear measuring tool. We determined the foveal thickness by averaging a horizontal and vertical scan passing through the foveal center.

Statistical analysis

All statistical analyses were carried out using JMP statistical discovery software (version 14.2.0; SAS Institute, Cary, NC). The paired t test was performed for comparison of two groups. Spearman correlation procedure was applied to investigate correlations between cone density and cumulative dose of HCQ at 24 months. Statistical significance was defined as $p < 0.05$.

(3) The relationship between vascular endothelial dysfunction and treatment frequency in neovascular age-related macular degeneration. (Study 3)

Patient selection

The inclusion criteria were (1) patients with a diagnosis of exudative age-related macular degeneration by clinical examination, fluorescein angiography (FA), and indocyanine green angiography (ICGA); (2) patients who underwent anti-VEGF monotherapy between January 2014 and December 2015; (3) patients with a minimum follow-up of 24 months. The exclusion criteria were (1) patients with a history of vitrectomy; (2) patients with end-stage AMD; (3) patients with other macular abnormalities such as myopic choroidal neovascularization (CNV), angioid streaks, or other secondary CNV; and (4) patients with a history of central serous choroidopathy (CSC). There were no exclusion criteria for history of photodynamic therapy, anti-VEGF therapy, or cataract surgery. If

patients had AMD in both eyes, the eye with a longer follow-up and greater number of injections was selected. If these were the same in both eyes, the right eye was selected. We enrolled and examined 159 consecutive patients with AMD who underwent EndoPAT measurement at Toyama University Hospital from January 2015. Of the 159 patients, 64 met the inclusion criteria. Seven patients with a history of vitrectomy, 78 patients with a follow-up of less than 24 months, 8 patients with end-stage AMD, and 2 patients with a history of CSC were excluded.

All patients underwent comprehensive ophthalmic examinations including measurement of best-corrected decimal visual acuity (BCVA), intraocular pressure, slit-lamp biomicroscopy, and optical coherence tomography (OCT) (RS-3000 Advance; Nidek, Aichi, Japan). FA and ICGA were performed before the first treatment and as needed. The classification of neovascular subtypes was performed according to the OCT, FA, and ICGA. The greatest linear dimension (GLD) was determined on the basis of the ICGA.

Treatment regimens

As the initial treatment, all the patients were given monthly intravitreal injections of ranibizumab (0.5 mg/0.05 mL) (Lucentis; Novartis, Bu¨lach, Switzerland) or aflibercept (2 mg/0.05 mL) (Eylea; Bayer Yakuhin, Osaka, Japan) until no signs of CNV activity were detected on OCT. After the initial treatment, the patients were followed monthly until any signs of exudation or new macular hemorrhage were detected. If we found signs of recurrence, we retreated them immediately and decided the next treatment according to the prediction made from the injection-retreatment interval. The patients were asked to visit before the next treatment to adjust the next injection interval. Treatments were extended by 2 weeks if no signs of recurrent exudation were detected. The treatment intervals were shortened by 2 weeks if any signs of exudation or new macular hemorrhage were detected. We provided the pro re nata (PRN) regimen as an option for patients whose injection-retreatment intervals were longer than 5 months. These patients were examined without treatment every 8 weeks; if we found intraretinal or subretinal fluid or new hemorrhage, we retreated them immediately. We tallied the number of anti-VEGF injections between January 2014 and December 2015. During this period, patients underwent anti-VEGF monotherapy.

PAT testing

Endothelial function was measured using the EndoPAT 2000. Thimble-like fingertip probes were applied to the finger of each patient's hand. An inflatable blood pressure cuff was placed on 1 upper arm. After a 5-min recording of baseline measurement, the blood

pressure cuff on the test arm was inflated to 60 mmHg above the baseline systolic blood pressure or to at least 200 mmHg for 5 min. The cuff was then deflated and finger arterial pulsatile volume changes were recorded from each finger for a further 5 min. PAT applies a significant counterpressure (70 mmHg) on the fingers and avoids distal venous distension, thereby preventing distal venous blood pooling and blood stasis, which could induce venoarteriolar reflex vasoconstriction. The pressure field also unloads arterial wall tension and increases the range of arterial wall motion without inducing potentially confounding vasomotor changes. The changes in finger blood volume after cuff release compared with baseline were analyzed with a computerized, automated algorithm. The calculated changes reflect the reactive hyperemia index (RHI), which is a measure of the endothelial response to occlusion and reactive hyperemia. The natural logarithmic scaled RHI (lnRHI) was calculated from the same ratio. The lnRHI has been shown to provide a better double-sided distribution that is closer to the normal distribution than does the RHI [8].

Statistical analysis

All statistical analyses were carried out using JMP statistical discovery software (version 11; SAS Institute, Cary, NC, USA). The Wilcoxon rank sum test or 1-way analysis of variance was performed to compare patient age, lnRHI, and number of injections. For assessing correlations between data including number of injections, lnRHI, and age, the weighted correlation coefficient was computed to adjust for aggregated data where each individual data point was weighted by its sample size. The associations between the systemic and ocular characteristics and the number of treatments were evaluated using univariate analysis. The characteristics with P<0.05 in the univariate analysis were entered into the multiple regression analysis. Statistical significance was defined as P<0.05.

(4) Using optical coherence tomography angiography to guide myopic choroidal neovascularization treatment: a three-year follow-up study. (Study 4)

Patient selection

This study was a retrospective, observational case series included 11 eyes of 11patients (3 men, 8 women) with myopic choroidal neovascularization (mCNV) who had been followed with OCTA for at least three years at Toyama University Hospital between

January 2016 and May 2020. Inclusion criteria were 1) a refractive error greater than -6.0D or an axial length $\geqq$ 26.5 mm which distinguished between mCNV and age-related macular degeneration, 2)the presence of subfoveal or juxtafoveal CNV, and 3) patients without advanced cataract, corneal opacity, or vitreous hemorrhage which disturbed to obtain OCTA images.

All patients underwent comprehensive ophthalmologic examinations, including measurement of the best-corrected visual acuity, intraocular pressure and axial length (OA-2000; TOMEY GmbH, Nagoya, Japan), slit-lamp biomicroscopy, color fundus photography, spectral domain OCT (RS-3000 Advance; NIDEK Co, Ltd, Aichi, Japan), and OCTA (RTVue XR Avanti; Optovue Inc., Fremont, CA, USA) at each visit.

Optical Coherence Tomography Angiography Analyses

OCTA volumes of 3×3 were obtained using the RTVue XR spectral domain OCT device (Optovue Inc., Freemont, CA, USA). We selected the outer retinal slab (from Bruch's membrane to inner nuclear/ outer plexiform layer junction) to identify the flow neovascular network of mCNV. In order to avoid segmentation error we used manual segmentation editing and propagation tool embedded into the OCTA device. CNV area was assessed by two experienced retina specialists (TUC and TO) in a masked manner confirmed by overlaying on B-scan images. Using the enface OCTA angiogram from each visit, readers independently measured the area. Measurements of the CNV area that differed by more than 10% were adjudicated through a second round of measurements. All measurements between the two readers were averaged.

CNV area was analyzed on en face OCTA images using Image J software Version 1.46r (National Institutes of Health, Bethesda, MD; available at http://imagej.nih.gov/ij/). The border of the CNV in the outer retinal slab was selected manually, then the area of CNV was estimated using the following equation: CNV area (mm^2) = CNV area (pixel)× $((3×AL /24.38 \text{ mm})/304 \text{ pixel})^2$. In this equation, Littmann's method [9] was performed for axial length (AL) adjustment: length (mm)=3×AL/24.38 (mm). Otsu algorism was applied for binary image processing [10,11]. Flow area of CNV was not calculated for small CNV which was less than 0.1mm2 since the value may potentially be inaccurate or biased.

Chorioretinal Atrophy Assessment

OCTA volumes of 6×6 were obtained using the RTVue XR spectral domain OCT device (Optovue Inc., Freemont, CA, USA). Atrophy was identified by a combination of review of en face OCT images for hyperreflective patches suggestive of increased signal

transmission, as well as scrutiny of overlaying on B-scan images. Three criteria had to be met for diagnosis of CRA on OCT based on previous wAMD studies [12,13]: (1) increased laser penetration into the choroidal and scleral tissue, (2) attenuation of the RPE band, and (3) collapse of thinning of the outer retinal layers. We calculated the areas of CRA using ImageJ software Version 1.46r (National Institutes of Health, Bethesda, MD; available at http://imagej.nih.gov/ij/). The border of the CRA in the custom slab was selected manually, then the area of CRA was estimated using the following equation: CRA area (mm^2) = CRA area (pixel) $\times$ (6$\times$AL /24.38 mm/604 pixel)^2.

Choroidal thickness measurement

Subfoveal choroidal thickness was manually segmented and defined as the distance from the retinal pigment epithelial (RPE) line to the chorioscleral interface. The observer measured the choroidal thickness using the caliper function built into the linear measuring tool. We determined the choroidal thickness by averaging a horizontal and vertical scan passing through the foveal center.

Treatment regimens

All patients were initially treated with monthly intravitreal injections of ranibizumab (0.5mg/0.05mL; Lucentis; Novartis, Bülach, Switzerland) or aflibercept (2mg/0.05ml; Eylea, Regeneron, Tarrytown, New York, USA) until no signs of CNV activity were detected on OCT including the fuzzy borders of CNV and subretinal hyperreflective exudation. Then patients were examined every 2 months without treatment. If we discovered intraretinal or subretinal hyporeflective or hyperreflective exudation, along with overlying fuzzy areas and absence of external limiting membrane visibility on OCT, we retreated them within one week. Occasionally, patients could not visit the hospital as planned because of poor health or other reasons. If recurrences had been identified frequently, fixed treatment or Treat and Extend (T&E) regimen was applied in compliance with patents' consent.

Results

(1) The association between cone density and visual function in patients with retinitis pigmentosa. (Study 1)

Clinical characteristics of the 6 patients (2 males and 4 females, mean [SD] age, 41.2 (14.7) years) are presented in Table 1. Case 1 was autosomal dominant and the other cases were sporadic.

Table 1 Clinical characteristics of retinitis pigmentosa (RP) patients at baseline

Case	Age (y)	Sex	Inheritance pattern	Eye	Decimal BCVA	Mean dB of central 4 points in HFA 10–2	Mean cone density at 0.5 mm from the foveal center (cells/mm^2)	Total foveal thickness (µm)
1	32	F	AD	R	1.2	35.0	3644 ± 2134	184
				L	1.2	33.5	4936 ± 4793	184
2	63	F	Sporadic	R	0.9	23.8	10,618 ± 3724	177
				L	1.0	20.8	8505 ± 3689	186
3	19	M	Sporadic	R	1.2	32.3	3644 ± 2134	132
				L	1.2	32.5	4936 ± 4793	141
4	44	F	Sporadic	R	1.2	34.3	15,759 ± 3121	261
				L	1.2	31.5	4674 ± 5551	257
5	45	M	Sporadic	R	1.2	34.5	15,841 ± 6386	209
				L	1.0	34.3	12,314 ± 5410	201
6	44	F	Sporadic	R	0.5	19.0	13,906 ± 2604	54
				L	0.5	24.3	15,371 ± 1970	67

Visual acuity

The visual acuities of cases 1, 2, 3, 4, and 5 were not changed over the 24-month study period, but the visual acuity of case 6 was decreased by more than 0.2 logMAR at 24 months, compared to the baseline value (Table 2).

Table 2 Changes in logMAR visual acuity of RP patients

Case		Baseline	6 months	12 months	18 months	24 months
1	R	− 0.079	0	0	− 0.079	− 0.079
	L	− 0.079	0	0	− 0.079	0
2	R	0.046	0	0	0.046	0.046
	L	0	0	0	0	0
3	R	− 0.079	− 0.079	0	0	− 0.079
	L	− 0.079	− 0.079	0	0	0
4	R	− 0.079	0.046	− 0.079	− 0.079	− 0.079
	L	− 0.079	− 0.079	− 0.079	0	− 0.079
5	R	− 0.079	− 0.079	− 0.079	0	− 0.079
	L	0	− 0.079	− 0.079	0	− 0.079
6	R	0.301	0.301	0.301	0.523	0.523 *
	L	0.301	0.301	0.398	0.523	0.699 *

*Visual acuity decreased more than 0.2 logMAR compared to the baseline

Cone density

AO images covered a 100 µm × 100 µm square area at 0.5 mm from the foveal center. The mean cone density at 0.5 mm from the foveal center was significantly decreased at 24 months in all eyes except for the left eyes of cases 4 and 5 (Table 3).

Table 3 Changes in mean cone density in each eye of RP patients (number/mm2)

Case		Baseline	6 months	12 months	18 months	24 months
1	R	3644 ± 2134	3180 ± 2137	3346 ± 3043	2228 ± 814	1267 ± 802
			(p = 0.523)	(*p* = 0.741)	(p = 0.1)	(*p* = 0.023)
	L	4936 ± 4793	4329 ± 2731	4141 ± 3803	1756 ± 689	1731 ± 649
			(*p* = 0.392)	(*p* = 0.342)	(*p* = 0.068)	(*p* = 0.039)
2	R	10,618 ± 3724	12,473 ± 1030	6882 ± 3090	6535 ± 2891	3619 ± 2976
			(*p* = 0.162)	(p = 0.004)	(*p* = 0.044)	(*p* = 0.006)
	L	8505 ± 3689	6370 ± 1311	5085 ± 2742	4050 ± 3008	2112 ± 1491
			(*p* = 0.85)	(*p* = 0.004)	(*p* = 0.005)	(*p* < 0.001)
3	R	3644 ± 2134	3180 ± 2136	3346 ± 3043	2228 ± 814	1267 ± 802
			(*p* = 0.523)	(*p* = 0.75)	(p = 0.1)	(*p* = 0.02)
	L	4936 ± 4793	4329 ± 2731	4141 ± 3803	1756 ± 688	1731 ± 649
			(*p* = 0.397)	(*p* = 0.354)	(*p* = 0.067)	(*p* = 0.04)
4	R	15,759 ± 3121	14,991 ± 3439	6824 ± 3735	11,861 ± 5469	7462 ± 2849
			(*p* = 0.4)	(*p* < 0.001)	(*p* = 0.007)	(*p* = 0.003)
	L	4674 ± 5551	6203 ± 4323	6747 ± 4984	10,282 ± 4180	4472 ± 4246
			(*p* = 0.115)	(*p* = 0.356)	(p < 0.001)	(*p* = 0.688)
5	R	15,841 ± 6386	8098 ± 7644	8881 ± 2058	9293 ± 2832	4734 ± 5561
			(p = 0.007)	(*p* = 0.008)	(p < 0.001)	(*p* = 0.018)
	L	12,314 ± 5410	16,498 ± 1790	14,096 ± 2847	11,851 ± 3783	10,996 ± 2588
			(*p* = 0.026)	(*p* = 0.389)	(*p* = 0.842)	(*p* = 0.571)
6	R	13,906 ± 2604	10,367 ± 3897	9499 ± 3964	4431 ± 3764	7462 ± 2849
			(*p* = 0.167)	(*p* = 0.071)	(p < 0.001)	(p < 0.001)
	L	15,371 ± 1970	15,918 ± 1526	12,530 ± 1973	9193 ± 2807	11,661 ± 1709
			(*p* = 0.128)	(*p* = 0.014)	(p < 0.001)	(p = 0.003)

OCT measurements

OCT at the fovea of all 6 patients showed interruption of the ellipsoid zone (EZ) and interdigitation zone (IZ). In each patient, changes in the thickness of the foveal center in the OCT image were examined over the 24-month study period. The thickness of the foveal center was not changed in either eye in cases 1, 2, 4, 5, and 6. Only the thickness of the foveal center in the eyes of case 3 showed a gradual decrease over the 24-months. The thickness of the foveal center in case 6 was significantly thinner than those of the other cases (p < 0.001) (Table 4).

Table 4 Changes in the thickness of the foveal center of RP patients (μm)

Case			Baseline	6 months	12 months	18 months	24 months
1	R	ILM-RPE	184	186	186	194	182
		ONL	98	99	95	101	99
		IS+OS	86	87	91	93	83
	L	ILM-RPE	184	190	186	190	185
		ONL	98	99	99	99	101
		IS+OS	86	91	87	91	84
2	R	ILM-RPE	177	180	186	190	185
		ONL	107	109	99	99	101
		IS+OS	70	71	87	91	84
	L	ILM-RPE	186	184	176	172	174
		ONL	116	113	109	105	107
		IS+OS	70	71	67	67	67
3	R	ILM-RPE	132	108	102	106	96
		ONL	74	58	53	53	54
		IS+OS	58	50	49	53	42
	L	ILM-RPE	141	117	115	117	110
		ONL	83	67	62	67	67
		IS+OS	58	50	53	50	43
4	R	ILM-RPE	261	265	265	262	260
		ONL	174	177	181	171	176
		IS+OS	87	88	84	91	84
	L	ILM-RPE	257	252	248	253	244
		ONL	168	168	168	173	164
		IS+OS	91	84	80	80	80
5	R	ILM-RPE	209	205	248	253	244
		ONL	113	168	168	173	164
		IS+OS	96	84	80	80	80
	L	ILM-RPE	201	206	202	205	203
		ONL	109	118	114	113	112
		IS+OS	92	88	88	92	91
6	R	ILM-RPE	54	57	46	50	54
		ONL	29	33	26	29	29
		IS+OS	25	24	20	21	25
	L	ILM-RPE	67	57	57	54	49
		ONL	42	37	41	42	37
		IS+OS	25	20	16	12	12

Mean sensitivity of central 2° × 2° of visual field

All patients underwent a visual field test of the central 10 degrees (Humphrey 10–2 program, Zeiss Meditec, CA) every 6 months over the 24 months. The mean sensitivity from dB of the 4 points at a 2° × 2° area centered at the fovea was calculated in each eye. The data are summarized in Table 5. The mean sensitivity of all cases was not changed over the study period (p = 0.17).

Table 5 Changes in mean sensitivity of the central 2° × 2° region of the visual field in RP patients (dB)

Case		Baseline	6 months	12 months	18 months	24 months
1	R	35.0	34.5	34.8	34.5	33.0
	L	33.5	33.8	35.3	35.0	34.3
2	R	26.0	27.3	25.8	25.5	24.0
	L	23.5	22.0	22.3	18.8	20.3
3	R	32.8	31.0	32.0	28.5	27.8
	L	33.5	32.0	30.5	24.8	28.5
4	R	34.3	30.0	34.5	35.0	34.5
	L	31.5	25.3	31.8	32.0	33.0
5	R	34.5	34.5	33.3	32.8	33.0
	L	34.3	34.3	32.3	29.5	31.8
6	R	19.0	12.3	16.0	16.3	13.0
	L	24.3	21.3	12.0	16.8	18.3

(2) Hydroxychloroquine's Early Impact on Cone Density. (Study 2)

Clinical characteristics and HCQ dosage information of the patients are presented in Table 6. Of the 29 patients, 28 were women. The mean age was 43.2±10.9 years. Twenty-eight patients were treated for SLE, and one patient was treated for dermatomyositis. The mean daily dose was 228±44.7 mg. The cumulative dose was 183±56.6g, on average, and the mean daily dose to real body weight ratio was 4.15±0.83 mg/kg. In 9 patients, the cumulative dose was over 200g in 2 years (Table 7). Mean daily dose-to-ideal body weight (IBW) was 4.06±0.73mg/kg, and there were no patients at this ratio >6.5mg/kg.

There was no correlation between cone density and cumulative dose of HCQ at 24 months (r=-0.0553, p=0.780).
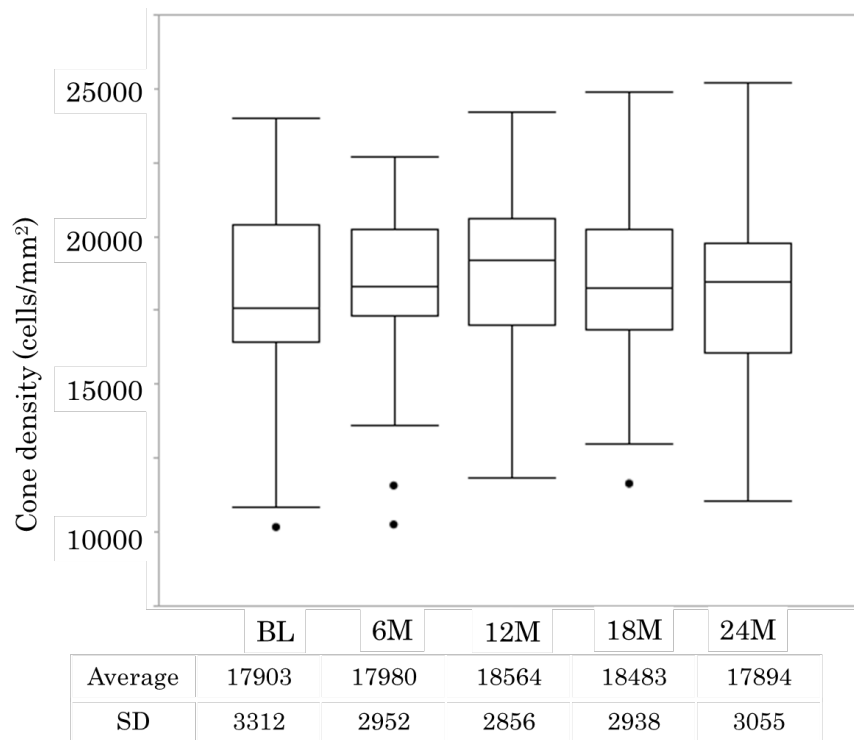
The mean cone density showed no significant change at 6, 12, 18, and 24 months compared with baseline (p=0.145, p=0.171, p=0.0973 and p=0.866, respectively) (Figure 2).

Table 6. Demographic Data and Clinical Characteristics of the Patients

Males:Females (%)	1:28 (3.4:96.6)
Mean $\pm$ age, y	43.2 $\pm$ 10.9
Diagnosis SLE:Dermatomyositis(%)	28:1(96.6:3.4)
Daily dose, mg	228 $\pm$ 44.7
Body-mass index, kg/m^2	21.9 $\pm$ 3.63
Ideal body weight, kg	56.1 $\pm$ 4.26
Daily dose/body weight, mg/kg	4.15 $\pm$ 0.83
Daily dose/ideal body weight, mg/kg	4.06 $\pm$ 0.73
Cumulative dose, g	183 $\pm$ 56.6
Cumulative dose/body weight, g/kg	8.51 $\pm$ 2.80

SLE, systemic lupus erythematosus

	BL	6M	12M	18M	24M
Average	17903	17980	18564	18483	17894
SD	3312	2952	2856	2938	3055

Figure 2: The mean cone density showed no significant change at 6, 12, 18, and 24

18

months compared with baseline (p=0.145, p=0.171, p=0.097 and p=0.866, respectively). (n=29)

Among 9 patients whose cumulative dose was over 200g in 2 years, the mean cone density showed no significant change at 6, 12, 18, and 24 months compared with baseline (p=0.381, p=0.380, p=0.281 and p=0.534, respectively) (Figure 3, Table 7). The mean foveal thickness at baseline, 6, 12, 18, and 24 months was 199.2±11.1, 199.1±11.0, 198.8±11.5, 199.8±11.0, and 198.2±11.0, respectively (mean±standard deviation (SD)). There was no significant change in the mean foveal thickness at 6, 12, 18, and 24 months compared with baseline (p=0.842, p=0.853, p=0.261 and p=0.375, respectively). BCVA at baseline, 6, 12, 18, and 24 months was -0.131±0.061, -0.133±0.048, -0.136±0.048, -0.133±0.053, and -0.137±0.053, respectively (mean±SD). BCVA showed no significant change at 6, 12, 18, and 24 months compared with baseline (p=0.824, p=0.617, p=0.756 and p=0.574, respectively).
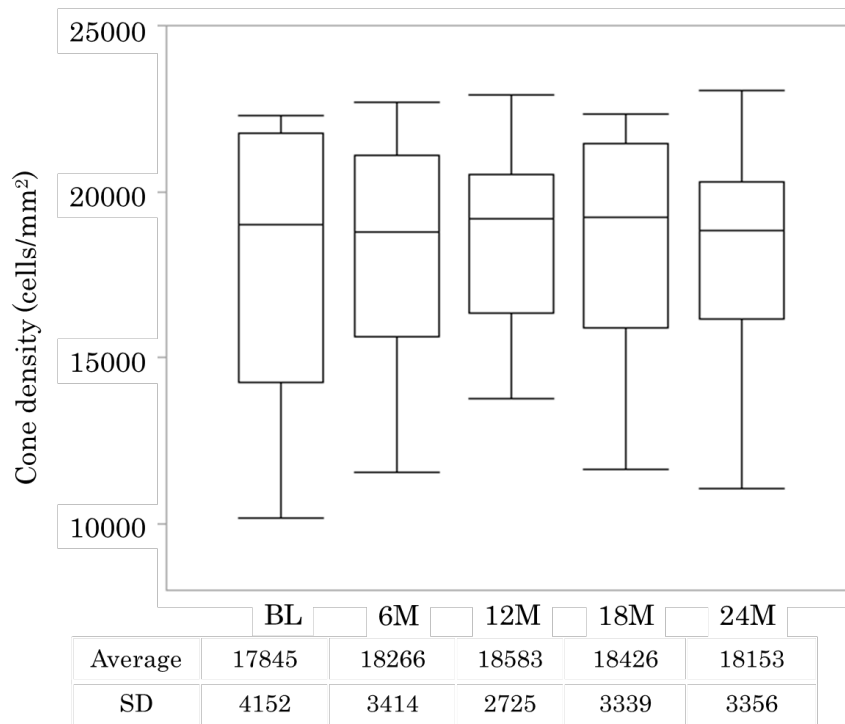

	BL	6M	12M	18M	24M
Average	17845	18266	18583	18426	18153
SD	4152	3414	2725	3339	3356

Figure 3: Among 9 patients whose cumulative dose was over 200g in 2 years, the mean cone density showed no significant change at 6, 12, 18, and 24 months compared with baseline (p=0.381, p=0.380, p=0.281 and p=0.534, respectively). (n=9)

Table 7. Demographics and adaptive optics findings of patients whose cumulative dose was over 200g in 2 years.

Patient number	Gender (M/F)	Age (years)	Cumulative dose in 2 years (g)	Pathology	Mean cone density (cells/mm^2)				
					baseline	6 months	12 months	18 months	24 months
1	F	46	339.6	SLE	19008+ 3229	18765+ 3870 (p=0.711)	19181+ 3481 (p=0.702)	18021+ 2696 (P=0.064)	18820± 3679 (p=0.621)
2	F	52	315.7	SLE	17007± 2248	18206± 2945 (P=0.202)	19518± 2382 (p=0.353)	19953± 1981 (p=0.290)	18873± 2322 (p=0.258)
3	F	45	275.1	SLE	22282± 2831	22685± 3169 (p=0.393)	22919± 2223 (p=0.513)	22320± 2399 (p=0.947)	23026± 1813 (p=0.476)
4	M	45	273.2	SLE	10156± 5397	13627± 3597 (p=0.292)	14752± 3209 (p=0.171)	11629± 4668 (p=0.471)	11050± 444 (p=0.860)
5	F	43	227.9	SLE	11507± 2761	11561± 1006 (p=0.974)	13756± 1809 (p=0.254)	14507± 2311 (p=0.125)	14082± 1580 (p=0.180)
6	F	55	226.2	SLE	22300± 1893	20691± 2924 (p=0.222)	18165± 2829 (p=0.058)	22081± 1949 (p=0.532)	20531± 2711 (p=0.248)
7	F	59	222.9	SLE	19566± 2145	19694± 2998 (p=0.823)	19993± 2497 (p=0.434)	19220± 2274 (p=0.481)	18709± 2122 (p=0.164)
8	F	3836	218.4	SLE	17581± 2923	17681± 2292 (p=0.934)	17893± 2674 (p=0.271)	17266± 1622 (p=0.866)	18218± 1621 (p=0.704)
9	F	38	203.2	SLE	21200± 2382	21486± 1638 (p=0.603)	21073± 1965 (p=0.734)	20840± 1058 (p=0.678)	20071± 869 (p=0.299)

(3) The relationship between vascular endothelial dysfunction and treatment frequency in neovascular age-related macular degeneration. (Study 3)

The characteristics of the 64 patients are presented in Table 1. The mean (SD) age was 76.0 ± 7.6 years, and 77% (49/65) of the patients were men. The mean lnRHI was 0.47 ± 0.17. The mean GLD was 3304 ± 926. The mean follow-up was 28.7 ± 21 months at baseline. Thirty-four patients (53%) had a history of PDT. During these 2 years, 10

patients (16%) received only ranibizumab, 44 patients (69%) received only aflibercept, and 10 patients (16%) received both ranibizumab and aflibercept. Of the 64 patients, 53 were treated with a modified treat and extend (TAE) regimen and 11, with a PRN regimen. The mean number of anti-VEGF injections between January 2014 and December 2015 was 8.2 ± 3.3 (Table 8).

Table 8 Demographics of the systemic and ocular characteristics and treatment factors in included eyes with age-related macular degen- eration (AMD)

No. of eyes	64
Age, years	76.0 ± 7.6
Male (%)	49 (77)
Body mass index, kg/m²	23.0 ± 2.6
Hypertension (%)	33 (52)
Diabetes mellitus (%)	8 (13)
HbA1c, %	7.2 ± 0.56
Smoking history (%)	43 (67)
Ex-smokers	29 (45)
Current smokers	14 (22)
Systolic blood pressure, mmHg	126 ± 16
Diastolic blood pressure, mmHg	77 ± 12
LnRHI	0.47 ± 0.17
No. of injections over 2 years	8.2 ± 3.3
GLD, 1m	3004 ± 926
Follow-up period (months) at baseline	28.7 ± 21
History of PDT (%)	34 (53)
Anti-VEGF agents (%)	
Ranibizumab only	10 (16)
Aflibercept only	44 (69)
Both	10 (16)
Treatment regimens (%)	
Modified TAE	53 (83)
PRN	11 (17)

Data are presented as means ± SDs or n (%)

RHI reactive hyperemia index, *LnRHI* natural logarithmic scaled RHI, *HbA1c* hemoglobin A1c, *GLD* greatest linear dimension, *PDT* pho- todynamic therapy, *VEGF* vascular endothelial growth factor, *TAE* treat and extend, *PRN* pro re nata

The mean number of injections was 9.0 ± 3.0 in the modified TAE regimen and 3.8 ± 1.1 in the PRN regimen. The lnRHI correlated with the number of anti-VEGF injections (r = -0.56; P = 0.030) (Figure 4). Age and number of injections were not correlated (r = 0.32; P = 0.24) (Figure 5). The lnRHI and age were weakly correlated (r = -0.28; P = 0.023; n = 64) (Figure 6).
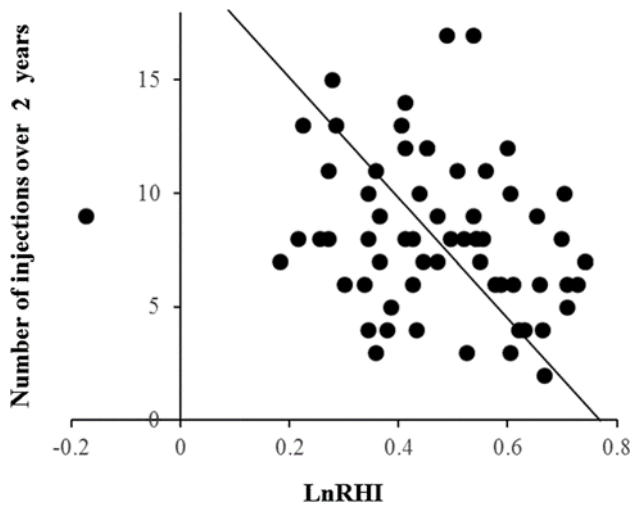
Figure 4 Scatterplot of the relation between the number of injections and natural logarithmic scaled reactive hyperemia index (lnRHI). The lnRHI correlated with the number of anti-VEGF injections (r = -0.56; P = 0.030). The solid line indicates the regression line. y = 20.38-25.89x; R^2 = 0.3126
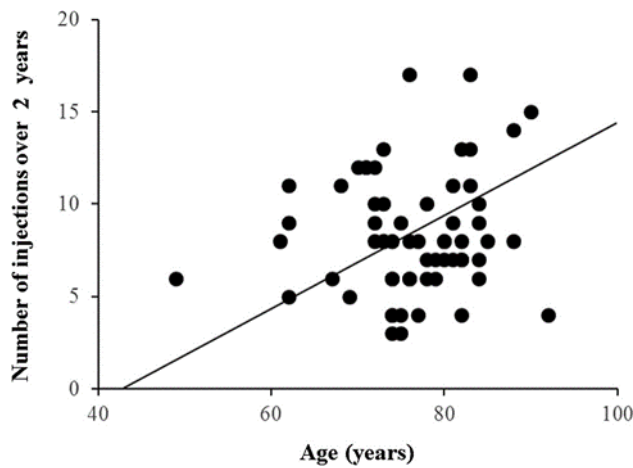
Figure 5 Scatterplot of the relation between the number of injections and age. The number of injections and age were not correlated (r = 0.32; P = 0.24). The solid line indicates the regression line. y = -10.98 + 0.2518x; R^2 = 0.1050
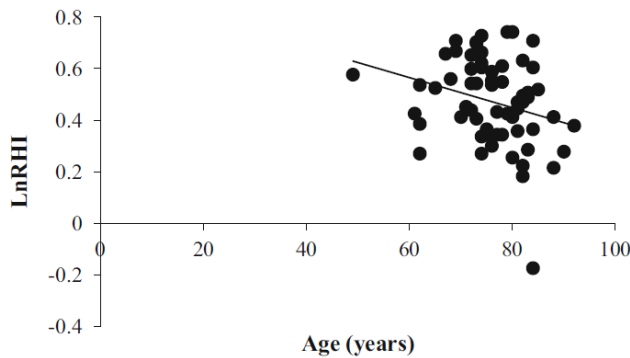

Figure 6 Correlation between age and natural logarithmic scaled reactive hyperemia index (lnRHI). The lnRHI and age were weakly correlated (r = -0.28; P = 0.023)

The mean lnRHI did not vary notably, owing to patient histories including smoking, hypertension, diabetes mellitus, stroke, and cardiovascular disease (P = 0.95, 0.087, 0.17, 0.25 and 0.61, respectively) (Table 9). Among the neovascular subtypes, the mean lnRHI did not differ significantly (P = 0.30). No marked difference was detected in the mean number of injections depending on the histories of smoking, hypertension, diabetes mellitus, stroke, and cardiovascular disease (P = 0.95, 0.71, 0.37, 0.69, and 0.34, respectively). Among the neovascular subtypes, the mean number of anti-VEGF injections did differ significantly (P = 0.0040).

The univariate analysis for the systemic and ocular characteristics associated with the number of treatments revealed that the lnRHI, neovascular subtypes, and

treatment regimens were significantly related to the number of injections (Table 10). The multiple regression analysis revealed that the lnRHI, neovascular subtypes, and treatment regimens were significantly associated with the number of treatments (Table 10).

Table 9 EndoPAT index and number of injections according to the clinical characteristics

Characteristics	No. of eyes (N = 64)	Age, years	LnRHI	No. of injections
Smoking history (%)				
No	21 (33)	77.7 ± 5.8	0.46 ± 0.20	8.0 ± 3.1
Yes	43 (67)	75.2 ± 8.2	0.48 ± 0.15	8.2 ± 3.4
P value[a]		0.34	0.95	0.95
Hypertension (%)				
No	31 (48)	75.0 ± 8.2	0.50 ± 0.18	8.0 ± 3.5
Yes	33 (52)	77.0 ± 6.8	0.44 ± 0.14	8.3 ± 3.2
P value[a]		0.39	0.087	0.71
Diabetes mellitus (%)				
No	56 (88)	76.4 ± 7.8	0.46 ± 0.17	8.3 ± 3.4
Yes	8 (13)	73.5 ± 4.6	0.54 ± 0.10	7.3 ± 2.8
P value[a]		0.15	0.17	0.37
History of stroke (%)				
No	56 (88)	75.9 ± 7.7	0.48 ± 0.17	8.1 ± 3.4
Yes	8 (13)	76.9 ± 6.6	0.42 ± 0.08	8.4 ± 3.0
P value[a]		0.83	0.25	0.69
Cardiovascular disease (%)				
No	61 (95)	76.0 ± 7.5	0.47 ± 0.17	8.1 ± 3.3
Yes	3 (5)	76.0 ± 8.5	0.52 ± 0.13	10.3 ± 3.9
P value[a]		0.67	0.61	0.34
Neovascular subtype				
Typical AMD		74.2 ± 9.2	0.45 ± 0.18	7.0 ± 2.5
PCV	30 (47)	77.3 ± 5.1	0.51 ± 0.16	8.7 ± 3.6
RAP	5 (8)	79.4 ± 7.1	0.41 ± 0.10	11.8 ± 2.0
P value[b]		0.18	0.30	0.0040

Data are presented as means ± SDs or n (%)

RHI reactive hyperemia index, LnRHI natural logarithmic scaled RHI, PCV polypoidal choroidal vasculopathy, RAP retinal angiomatous proliferation

24

a Wilcoxon rank sum test

b 1-way analysis of variance

Table 10 Clinical characteristics and treatment factors associated with the number of treatments

	Standardized coefficient beta	Standard error	T ratio	P value
Univariate analysis				
LnRHI	−0.27	2.3	−2.2	0.030
Age, years	0.18	0.055	1.5	0.15
Smoking history	0.026	0.90	0.21	0.84
Hypertension	0.041	0.85	0.32	0.75
Diabetes mellitus	−0.10	1.3	−0.83	0.41
History of stroke	0.074	1.2	0.58	0.56
Cardiovascular disease	0.14	2.0	1.1	0.26
Sex, male	−0.038	1.0	−0.30	0.77
GLD	0.026	0.00038	0.20	0.40
Follow-up period at baseline	−0.035	0.020	−0.28	0.78
Neovascular subtype				
Typical AMD	Reference			
PCV	0.27	0.81	2.2	0.0163
RAP	0.39	1.5	3.2	0.0033
Treatment regimens (modified TAE)	0.53	0.95	5.0	\0.001
Anti-VEGF agents				
Ranibizumab only	Reference			
Aflibercept only	0.065	1.2	0.39	0.70
Both	−0.033	1.5	−0.20	0.84
Multiple regression analysis				
LnRHI	−0.21	2.0	−2.0	0.047
Neovascular subtype				
Typical AMD	Reference			
PCV	0.24	0.70	2.2	0.029
RAP	0.30	1.3	2.9	0.0055
Treatment regimens (modified TAE)	0.45	0.90	4.4	\0.001

RHI reactive hyperemia index, LnRHI natural logarithmic scaled RHI, GLD greatest linear dimension, PCV polypoidal choroidal vasculopathy, RAP retinal angiomatous proliferation, TAE treat and extend

(4) Using optical coherence tomography angiography to guide myopic choroidal neovascularization treatment: a three-year follow-up study. (Study 4)

The patients' ages at baseline ranged from 59 years to 82 years (mean±SD, 70.8±6.7 years). The mean follow-up period after clinical onset of the CNV at baseline was 9.3±15 months (range, 0 to 49 months). Four patients (case 5, 7, 8 and 10) had a history of treatments against mCNV prior to undergoing OCTA. The baseline characteristics are listed in Table 11. The number of recurrences and treatments and anti-VEGF drugs are listed in Table 12.

Cases 7, 8 and 10 did not exhibit recurrences during the three years and did not show remarkable changes in the size of CNV without any treatments (Table 12, Figure 7). In case 5, we performed OCTA for the first time when we detected a recurrence 28 months after the first treatment. After three injections, the size of CNV decreased and stabilized thereafter (Figure 7).

Seven patients (cases 1,2,3,4,6,9 and 11) were treatment naïve at baseline. In three cases (cases 1,2 and 3), the size of CNV had increased over three years (Figure 7). In each case, recurrences were detected once, four times and four times respectively during the three years (Table 2). In case 1, recurrence was detected 16 months after first treatments and was treated with ranibizumab one week later. In cases 2 and 3, the treatments for the third and the first recurrences could not be administered promptly. The intervals between follow-up visits were four months and five months respectively when we detected those recurrences because the patients were unable to get to the hospital. Without immediate treatments, the size of CNV increased in both cases (CNV size before the recurrence, 0.130mm2 and 0.212mm2; CNV size after the recurrence, 0.233mm2 and 0.640mm2, respectively) (Figure 7).

In cases 4 and 6, the size of CNV decreased over the three years (Figure 7). In case 4, no recurrences were identified after first treatments including two injections. In case 6, we detected recurrences three times during the first year. The intervals between the treatments and the recurrences were less than 8 weeks. We started to inject anti-VEGF drugs every 6 weeks for 10 months. During the ten months, no recurrence was detected

and we resumed pro re nata regimen. The total number of treatments was eleven (Table 12).

Cases 9 and 11 did not show remarkable changes in the size of CNV during the three years (Figure 7). In case 9, the first recurrence was detected only three months after first treatment of consisting of monthly injections of ranibizumab. The second recurrence was identified less than 8 weeks later. We started T&E regimen and continued for one and a half years. Since we detected no recurrences during the regimen, we restarted the pro re nata regimen. No recurrence was found; the total number of injections was eleven (Table 12). In case 11, we detected a single recurrence 10 weeks after the first treatment and did not detected any recurrences thereafter.

The size of CRA had increased obviously during the three years in cases 5, 6 and 7 (Figure 7). Those cases had larger size of CNV at baseline compared to others (Table 13). There was a correlation between mCNV enlargement and CRA size at 3 years (Spearman correlation coefficients, r = 0.846; p=0.002; n=11); a larger sample size would be needed to consider this result statistically significant. In case 6, visual acuity deteriorated due to the progression of CRA (Table 14).

In cases 6 and 9, the foveal choroidal thickness (CT) decreased to 52.6% and 62.1% of baseline CT respectively in three years. Both cases underwent injection therapy 11 times during the course of the study (Table 13).

Table 11.　Baseline Characteristics in 11 Cases

Case	Age	Sex	R/L	Axial length (mm)	VA	Location	Size of CNV (mm^2)
1	76	F	L	32.0	0.8	juxta	0.166
2	80	M	R	31.1	0.2	subfovea	0.142
3	82	F	L	27.0	0.2	subfovea	0.196
4	59	F	R	29.1	0.4	juxta	0.328
5*	74	F	L	27.7	0.4	subfovea	0.41
6	67	M	L	28.9	0.2	subfovea	0.814
7*	70	F	R	27.8	0.7	juxta	0.908
8*	66	F	L	29.4	0.9	juxta	0.121
9	73	F	R	29.4	0.5	juxta	0.235
10*	69	M	R	28.1	0.3	juxta	0.212
11	63	F	L	29.1	0.5	juxta	0.316

F, female; M, male; L, left; R, right; CNV, choroidal neovascularization; CRA, chorioretinal atrophy; CT, choroidal thickness; IVB, intravitreal injection of

bevacizumab; IVA, intravitreal injection of aflibercept; IVR, intravitreal injection of ranibizumab; VA, visual acuity

*patient with a history of treatments

Table 12. Recurrences and Treatments over three years

Case	Number of recurrences (1st /2nd /3rd)	Number of treatments (1st /2nd /3rd)	IVR/IVA
1	1 (0/1/0)	3 (2/1/0)	3/0
2	4 (2/1/1)	5 (2/2/1)	5/0
3	4 (1/1/2)	6 (3/1/2)	6/0
4	0	2 (2/0/0)	2/0
5	1 (1/0/0)	3 (3/0/0)	3/0
6	3 (3/0/0)	11 (7/4/0)	7/4
7	0	0	0/0
8	0	0	0/0
9	2 (2/0/0)	11 (6/4/1)	7/4
10	0	0	0/0
11	1 (1/0/0)	7 (6/1/0)	7/0

1st, first year; 2nd, second year; 3rd, third year; IVR, intravitreal injection of ranibizumab; IVA, intravitreal injection of aflibercept

Table 13. Changes of the CNV Size, CRA Size and CT

Case	Size of CNV at baseline (mm²)	Size of CNV at 3 years (mm²)	Size of CRA at baseline (mm²)	Size of CRA at 3 years (mm²)	% of CRA in proportion to the baseline	CT at baseline (μm)	CT at 3 years (μm)	% of CT in proportion to the baseline
1	0.166	0.220	14.8	16.6	112	34.0	32.0	94.1
2	0.142	0.272	15.8	16.7	106	10.0	12.0	120
3	0.196	0.604	0	0	100	16.0	15.5	96.9
4	0.328	0.269	0	0	100	64.0	56.5	88.3
5	0.41	0.191	4.08	8.16	200	29.0	25.0	86.2
6	0.814	0.460	0	3.57	*	66.5	35.0	52.6
7	0.908	0.903	1.49	3.63	244	38.0	38.5	101
8	0.121	0.101	0	0	100	19.0	14.5	76.3
9	0.235	0.231	0	0	100	72.5	45.0	62.1
10	0.212	0.231	0	0	100	40.5	39.0	96.3
11	0.316	0.292	0	0	100	44.5	37.0	83.1

CNV, choroidal neovascularization; CRA, chorioretinal atrophy; CT, choroidal thickness

*, CRA occurred during the first year

Table 14. Changes of Visual Acuity in three years

Case	VA at baseline	VA at 3 years
1	20/25	20/32
2	20/100	20/100
3	20/100	20/63
4	20/50	20/16
5	20/50	20/63
6	20/100	20/630
7	20/32	20/32
8	20/25	20/25
9	20/40	20/32
10	20/63	20/63
11	20/40	20/20

VA, visual acuity

Figure 7-a

Flow area of mCNV (mm²) — case 1, case 2, case 3 at baseline, 1Y, 2Y, 3Y

Figure 7-b

Flow area of mCNV (mm²) — case 4, case 5, case 6 at baseline, 1Y, 2Y, 3Y

Figure 7-c

Flow area of mCNV (mm²) — case 7, case 8, case 9, case 10, case 11 at baseline, 1Y, 2Y, 3Y
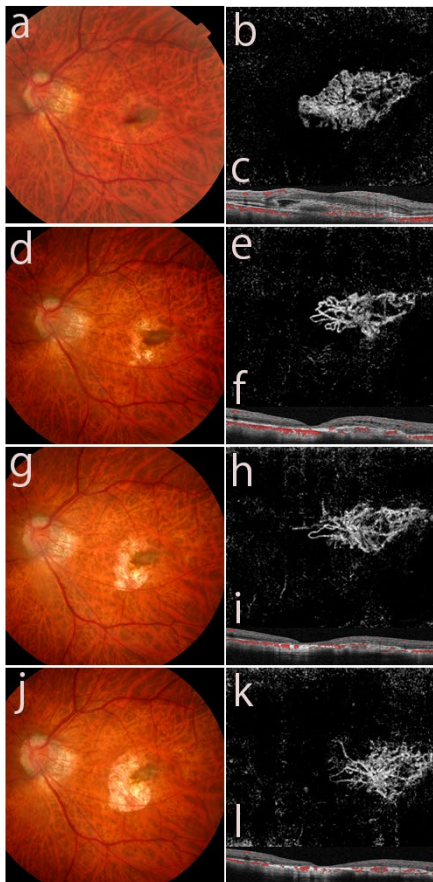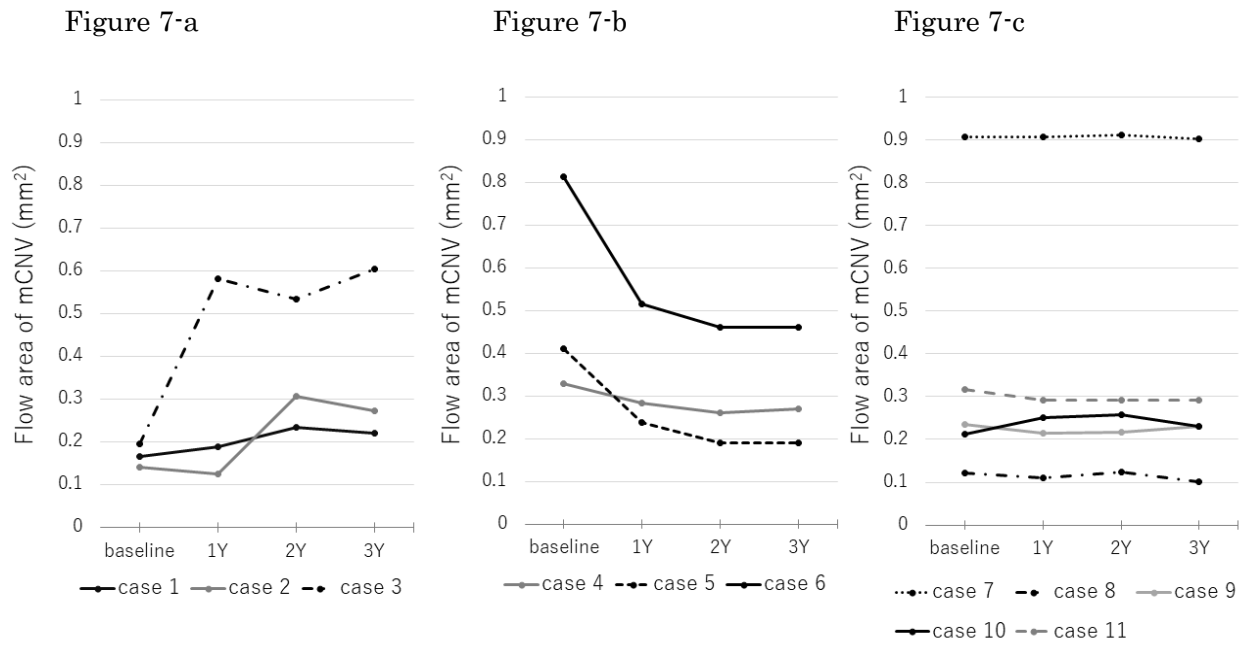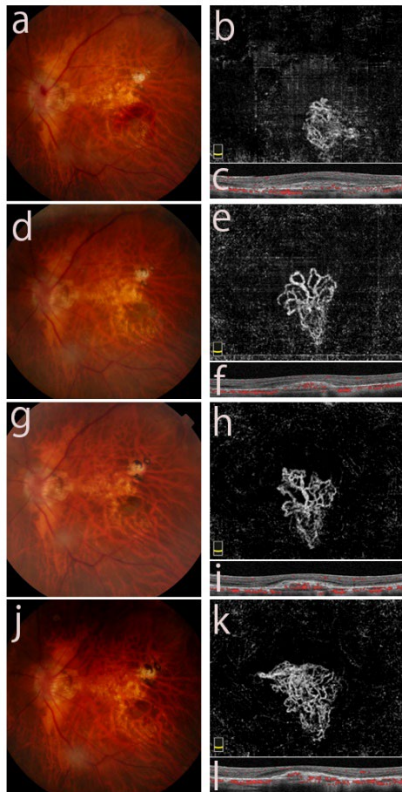

Figure 8 Patient 6. a, b and c: baseline; d, e and f: 1 year; g, h and i: 2 year; j, k and l: 3

year. Fundus photographs (a, d, g and j) show development and enlargement of CNV-related macular atrophy (arrow). b, The OCTA image shows the presence of mCNV in the outer retinal layer. The lesion is composed by numerous tiny capillaries. c, Correlated OCT B-scan shows active mCNV lesions including fuzzy borders of CNV and subretinal hyperreflective exudation. e, h and k, The OCTA images display an irregular-shaped neovascular network with mature, large vessels. f, i and l, Correlated OCT B-scans show a well-defined profile with hyperreflective borders and increased laser penetration into the choroidal and scleral tissue (arrow)

Figure 9 Patient 3. a, b and c: baseline; d, e and f: 1 year; g, h and i: 2 year; j, k and l: 3 year. Fundus photographs (a, d, g and j) show patchy atrophy close to macula (arrow) and no development of CNV-related macular atrophy. b, The OCTA image reveals the presence of mCNV in the outer retinal layer. The lesion is poorly defined and composed by numerous tiny capillaries. c, Correlated OCT B-scan shows active mCNV lesions including fuzzy borders of CNV and subretinal hyperreflective exudation. e, h and k, The OCTA images expose an irregular-shaped neovascular network with mature, large vessels. f, i and l, Correlated OCT B-scans show a well-defined profile with hyperreflective borders
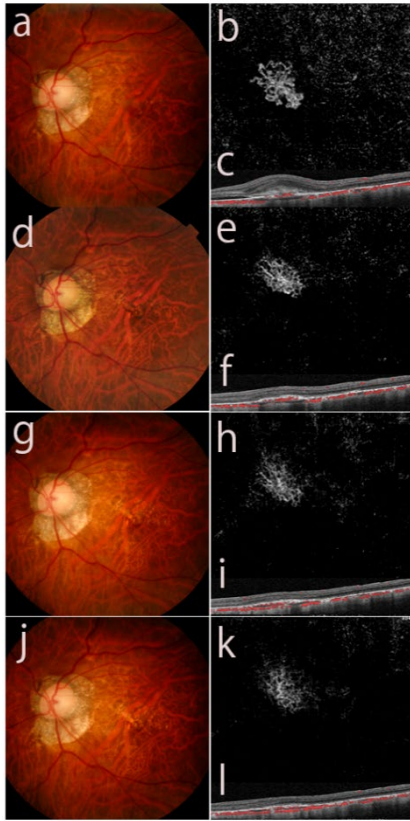
Figure 10 Patient 11. a, b and c: baseline; d, e and f: 1 year; g, h and i: 2 year; j, k and l: 3 year. Fundus photographs (a, d, g and j) uncover no development of CNV-related macular atrophy. b, The OCTA image shows the presence of mCNV in the outer retinal layer. The lesion is medusa shaped and well defined. c, Correlated OCT B-scan shows active mCNV lesions including fuzzy borders of CNV and subretinal hyperreflective exudation. e, h and k, The OCTA images show poorly defined mCNV in the outer retinal layer. f, i and l, Correlated OCT B-scans show a well-defined profile with hyperreflective borders

Discussion

Study 1 revealed that the cone photoreceptors decreased in all RP patients over 2 years. Five of six RP patients, however, did not show remarkable changes in visual acuity, foveal sensitivity, or the IS+OS thickness of the foveal center. Adding assessment of cone loss to standard clinical test (e.g. visual acuity, visual filed and OCT) may shorten the period required to accurately predict the rate of progression of macular degeneration.

A novel finding in Study 2 was that there was no significant decrease in cone density in first 2 years of HCQ use. Visual acuity and foveal thickness did not show obvious change, either. AO fundus camera may provide us with valuable information on the natural history of cone survival in macular degeneration. Study 1 and Study 2 together, AO fundus camera may enable us to monitor the onset and progression of macular degeneration more sensitively and to protect patients' vision.

Study 3 demonstrated that the endothelial dysfunction correlates with the number of anti-VEGF injections for nAMD. This finding suggests that improving endothelial function may reduce the recurrence of nAMD. Study 4 showed that it is essential to treat mCNV recurrence as soon as possible to prevent enlargement of mCNV which might cause severe visual impairment due to macular degeneration secondary to mCNV. From Study 3 and 4, we propose that improving endothelial function will reduce the risk of the reccurrence of CNV, and once CNV reoccurs, prompt treatment is critical to suppress the enlargement of CNV which might cause the progression of macular degeneration.

(1) The association between cone density and visual function in patients with retinitis pigmentosa. (Study 1)

This study was the first to report the changes in the numbers of cone photoreceptors at the same location, 0.5 mm from the foveal center, over a period of 2 years; the results showed that the cone photoreceptors were decreased in all RP patients. In RP, the photoreceptors are primarily affected, and disruption of the inner segment ellipsoid is found using OCT images. AO is useful for counting cone photoreceptors directly and detecting photoreceptors abnormalities in earlier stages of RP. AO may shorten the period required for accurate prediction of the rate of progression of RP.

There has been an increased interest in the retinal photoreceptor structure in RP. Several studies have suggested that cone density is decreased in RP patients. AO has revealed that cone patterns were abnormal in eyes with inherited forms of retinal degeneration, including conerod dystrophy, Stargardt disease, and RP [14,15]. Sun et al. found that foveal cone density was reduced by 38% from normal before visual function was affected, without any visible findings on OCT [16]. Ratnam et al. reported that cone density was reduced by up to 62% below normal in eyes with visual acuity and sensitivity that remained within normal limits [17].

Our present study was the first to investigate the changes in cone density at the

same location over 2 years in RP patients. As previously reported, visual acuity is correlated with the mean deviation of the Humphrey central 10–2 program in RP patients [18]. We thus used the 10–2 SITA standard program to evaluate foveal sensitivity. Rangaswamy et al. reported that loss of visual field sensitivity was linearly related to a decrease in photoreceptor thickness in RP patients [19]. Therefore, we measured not only the total foveal thickness but also the thickness of the outer nuclear layer and the thickness of the IS+OS at the center of the fovea and assessed the relationship between these measurements and the foveal sensitivity.

Five of six RP patients in our study did not show remarkable changes in visual acuity, foveal sensitivity, or the IS+OS thickness of the foveal center despite showing a decrease of cone density over the 2-year study periods. This finding agrees with a previous study in which, the cone mosaic was found to be disrupted in the eyes of RP patients even when visual acuity and foveal sensitivity were good [20]. There were several reasons for the discrepancy between visual acuity and cone density in the current study.

First, we performed cone counting at 0.5 mm from the foveal center, not at the very center of the fovea. A previous study reported that the cone density is high at the foveal center and it varies widely among individuals (100,000–324,000 cones/mm2) [21]. Therefore, we did not have sufficient resolution to distinguish individual cone mosaic at the foveal center using an AO fundus camera. Another explanation for the discrepancy may be that there is redundancy in the macula. Previous studies using animal models found that a neural remodeling process occurs following cone loss [22]. Because there is redundancy in the macula, a greater receptive overlap would permit patients to sustain structural change or cell loss before significant functional changes [23]. Two years may not be a sufficient period to predict the rate of disease progression with visual field testing and OCT images. A longitudinal follow-up to the current study is thus needed to analyze the association between retinal structure and function in RP patients.

(2) Hydroxychloroquine's Early Impact on Cone Density. (Study 2)

A novel finding in our study was that there was no significant decrease in cone density in first 2 years of HCQ use. VA and foveal thickness did not show obvious change, either. To the best of our knowledge, this is the first prospective study on analysis of the cone density in initial stage of HCQ introduction using AO.

Stepien et al. found irregularities in the cone density in areas with normal

Humphrey visual field (HVF) 10-2 and SD-OCT findings [24]. This finding indicated potential use of AO as an essential tool for detecting the preclinical stage of HCQ toxicity. Debellemaniere et al. also reported that cone loss may occur at an early stage after exposure to HCQ without clinically evident toxicity. They showed a significant negative correlation between parafoveal cone density and cumulative HCQ dose (r2=0.23, p=0.0018) in patients with no clinical evidence of maculopathy. In 18 of 23 patients, the cumulative dose was over 200g [25]. In the current study, there was no correlation between cone density and cumulative dose of HCQ at 24 months (r=-0.0553, p=0.780). It might be due to the smaller number of patients whose cumulative dose was over 200g (9 of 29 patients). AO may provide us with valuable information on the natural history of cone survival exposed to HCQ. Since retinal degeneration from HCQ can continue to progress even after the drug is discontinued, detecting early retinopathy is essential. HCQ cessation, however, handicaps patients with autoimmune disease because alternatives to HCQ are more expensive and have more side effects [26,27]. We need to balance managing autoimmune disease and minimizing the risk of HCQR. Adding assessment of cone loss to standard clinical test (e.g., fundus photograph, HVF and SD-OCT) may enable us to monitor HCQR more sensitively. Precise monitoring helps both screening ophthalmologists and prescribing physicians not only for HCQ cessation but also for raising the possibility of reducing daily dosing before drug cessation. It also allows for balancing controlling a systemic disease with protecting patients' vision.

There are potential limitations in this study such as relatively small sample size and gender bias as most of our patients were females. Some limitations were also intrinsic to detecting cone loss because it is still difficult for AO to distinguish cone damage from artifact. Media opacities and dry eye disease which leading to tear film instability and keratitis cause poor image quality. The locations where AO measures with enough reliability and repeatability are still limited. In the current study, cone density was measured in 4 quadrants (nasal, temporal, superior, and inferior) at 0.75mm from the foveal center. In some Asian patients, however, researchers found pericentral retinopathy eight degrees or more from the center of the fovea[28,29]. Technical improvements are still needed to acquire AO images in patients on a HCQ regimen. A longitudinal follow-up to the current study is needed to obtain useful information on the long-term cone survive exposed to HCQ.

(3) The relationship between vascular endothelial dysfunction and treatment frequency in neovascular age-related macular degeneration. (Study 3)

The present study demonstrated for the first time that endothelial dysfunction correlates with the number of anti- VEGF injections for nAMD. This finding suggests that endothelial dysfunction is associated with the length of the effect of anti-VEGF treatment. Measurement of endothelial function using the EndoPAT2000 may help to predict the therapeutic response to anti-VEGF therapy.

The EndoPAT2000 is a useful method for assessing endothelial function and is easily performed at the outpatient clinic. It measures peripheral vasodilator response with fingertip pulse amplitude tonometry after ischemia. Nitric oxide produced by endothelium plays a central role in vasodilation during reactive hyperemia [30]. In addition to stimulating vasodilation, nitric oxide has antiatherogenic properties such as antiinflammatory and antithrombotic properties [31]. Measurement of the increase in digital blood volume during reactive hyperemia using the Endo-PAT2000 is a convenient test of nitric oxide bioavailability.

The RHI, consistent with endothelial function, has been shown to be related to multiple traditional and metabolic cardiovascular risk factors including age, sex, BMI, smoking, diabetes mellitus, and dyslipidemia [32]. In our study, the lnRHI and age were negatively correlated. In the presence of these risk factors, endothelial cells undergo phenotypic changes resulting in decreased nitric oxide bioactivity, thereby promoting vasoconstriction, inflammation, and thrombosis [31]. Endothelial dysfunction is a key step in the development of atherosclerosis and contributes to the development of cardiovascular disease [33]. A low RHI detected by the EndoPAT2000 was associated with a higher rate of cardiovascular adverse events (cardiac death, myocardial infarction, revascularization, or cardiac hospitalization) [34]. And the lnRHI was reported to be an independent predictor of cardiovascular adverse events [31].

Cardiovascular risk factors have been also identified as risk factors for AMD [35]. Snow and Seddon suggested that AMD and cardiovascular disease share common risk factors and probably a common pathogenesis [36]. Recently, attention has been focused on the similarity of AMD and atherosclerosis, and relationships between endothelial dysfunction and AMD have been revealed [37]. The Beaver Dam Eye Study reported that soluble vascular cell adhesion molecule-1 was modestly associated with the 20-year cumulative incidence of early AMD [38]. Machalinska et al. suggested that endothelial alteration accompanies AMD and that circulating endothelial progenitor cells and endothelial cells, together with endothelin-1, might play an important role in the process of CNV development at sites of local retinal ischemia [39].

A correlation between the mean lnRHI and frequency of anti-VEGF treatment

indicates that endothelial dysfunction is associated with CNV reactivation. Nitric oxide is constitutionally expressed in normal endothelium and has vasodilatory, antiinflammatory, and antithrombotic properties. Endothelial dysfunction results in decreased nitric oxide bioactivity, promoting vasoconstriction, inflammation, and thrombosis [31,32]. This may lead to local retinal ischemia, which promotes the development and reactivation of CNV in AMD.

Chronic AMD demands continual treatment or monitoring visits and places a heavy burden on patients and institutions. It would be helpful for patients, patient families, and medical staff to be able to predict the number of anti-VEGF treatments. In the present study, the lnRHI, neovascular subtypes, and treatment regimens were significantly associated with the number of anti-VEGF treatments over 2 years. Kuroda et al. reported that recurrence of nAMD was observed significantly more in older and male patients during the first year and that eyes with PCV had a shorter interval of recurrence after the initial treatment than did eyes with typical AMD [40]. The findings of the present report are consistent with those findings and showed that endothelial function and subtypes of nAMD were associated with the effect of anti-VEGF treatment in the maintenance phase.

The potential limitations of this study include its retrospective nature, relatively small sample size, and use of different anti-VEGF agents. Patients with different followup periods and previous treatments were also included in the study. Some limitations were intrinsic to tallying the number of injections because their number did not always reflect the exact intervals of recurrence. Both the modified TAE regimen and the PRN regimen were adopted in the maintenance phase to avoid the possibility of overtreatment or of undertreatment. A recent prospective study showed that need of retreatment follows a relatively rhythmic pattern [41]. This result supports the validity of the modified TAE regimen. However, it becomes more difficult to predict the time of recurrence as the injection-retreatment intervals lengthen. For patients whose intervals of recurrence are long, the number of injections following the PRN regimen might be closer to the real number of recurrences. Therefore, including both regimens in the maintenance phase seems reasonable. And it is presumable that a patient who has undergone a greater number of treatments has experienced a greater number of recurrences compared with a patient who has undergone a smaller number of treatments. Despite these limitations, we showed that endothelial function measured by the EndoPAT 2000 might help to predict frequency of anti-VEGF treatment in real-life clinical practice. Further prospective studies will be needed to determine the predictive value of endothelial function for treatment frequency.

(4) Using optical coherence tomography angiography to guide myopic choroidal neovascularization treatment: a three-year follow-up study. (Study 4)

In the current study, we observed eleven eyes with mCNV using OCTA for three years. Without recurrences, the size of CNV did not show remarkable changes in three years (cases 7, 8 and 10). Without prompt treatment, however, the size of CNV increased significantly (cases 2 and 3). We propose that it is essential to treat mCNV recurrence as soon as possible so to prevent enlargement of mCNV which might cause severe visual impairment due to CRA development secondary to mCNV.

Several studies identified that larger CNV size was one of the risk factors of vision loss due to the progression of CRA [42,43]. Kasahara et al reported on the 6-year outcome of intravitreal bevacizumab in eyes with mCNV. The best corrected visual acuity at 6 years was significantly correlated with the baseline CNV size and the size of CNV-related macular atrophy at 6 years [42]. Kojima et al showed that CNV size and older age were important factors in the development of CRA [43]. Consistent with these reports, the present study showed CRA progression in patients whose CNV size was large at baseline and enlarged over the three-year study period (case 5, 6 and 7). Since CNV size may influence the development and the progression of CRA, it is critical to understand how the CNV size changes over time. OCTA allows highly detailed observation of the shape and size of CNV because there are no obscuring details due to dye leakage [44]. OCTA revealed that CNV changes noticeably after treatments with anti-VEGF agents in the short term [45,46]. Lumbroso et al. assessed Type 2 CNV 24 hours after anti-VEGF treatment and 7 days, 20 days and 30 days later [45]. They found a decrease of anastomosis and small capillaries, and some widening of the main vessels. Cheng et al found that selected CNV area and flow area were decreased thirty days after treatment [46]. The long-term changes of the mCNV size, however, has not been adequately assessed. In the current study, we showed the changes of the mCNV size over three years using OCTA. The CNV size had decreased after initial treatments with anti-VEGF drugs in the first period of the three years and remained stable thereafter without any recurrences (case 4 and 5). Decreasing CNV size and inhibiting its growth may prevent the development and enlargement of CRA. To suppress CNV enlargement, recurrences should be treated as soon as possible. In cases 2 and 3, the follow-up intervals were 4 months and 5 months respectively when we found reactivation of CNV. Since the

recurrences were not treated immediately, the CNV markedly increased in size (163% and 275%, respectively). In contrast, prompt treatments against recurrences inhibited enlargement of the CNV in the long term (case 1, 5, 6, 9 and 11). These results suggest that initial treatments reduce CNV size and regular examination at appropriate intervals and prompt treatments against recurrences are essential to regulate the size of CNV.

Many specialists consider thinning of the subfoveal choroidal thickness is also one of the risk factors for CRA [47] and mCNV recurrence [48]. Sayanagi et al reported that aflibercept was more effective for choroidal thickness reduction compared with ranibizumab at 1 year in eyes with mCNV [49]. Previous studies revealed that aflibercept decreased choroidal thickness more severely than ranibizumab in neovascular AMD [50] and it is concerning that aflibercept may exacerbate the development of macular atrophy by obstructing the choroidal circulation which plays a pivotal role in maintaining the outer retinal layer and retinal pigment epithelium(RPE). Frequency of injections was also reported as a risk factor for macular atrophy [51,52], though it is still controversial whether the number of injections is associated with the incidence of macular atrophy [53,54]. In the current study, cases 6 and 9 experienced severe thinning of the choroid at 3 years (Table 12). The largest number of injection therapies (11 times) were performed in these cases. From the standpoint of preventing choroidal thinning which could trigger CRA, we believe scrutinizing the effects of anti-VEGF agents and treatment frequency on choroidal thickness to be necessary.

The retrospective nature, small sample size and use of different anti-VEGF agents potentially limit the conclusions of this study. Further investigations with larger samples are warranted to confirm our observations. Patients with different follow-up periods and previous treatments were also included in this study. Some features of pathologic myopia such as posterior staphyloma and RPE/chorioretinal atrophy diminish OCTA image quality and interpretation. Manual segmentation to accurately locate the CNV lesion may induce inaccuracies. Despite these limitations, we believe our findings indicate that early detection and prompt treatment will lead to better care for patients in real-life clinical practice.

Conclusions

In macular degeneration, photoreceptor decrease occurs prior to visual impairment. An AO fundus camera may enable us to monitor photoreceptors decrease precisely and to forecast progression of macular degeneration accurately. To prevent photoreceptor loss in macular degeneration secondary to CNV, improving endothelial function may be an effective approach by reducing the reccurence of CNV. Once CNV reoccurs, prompt treatment is critical to prevent enlargement of CNV which might cause severe photoreceptor loss due to macular degeneration secondary to CNV.

References

1. Liang J, Williams DR, Miller DT (1997) Supernormal vision and high-resolution retinal imaging through adaptive optics. J Opt Soc Am A Opt Image Sci Vis 14: 2884–2892.

2. Roorda A, Williams DR (1999) The arrangement of the three cone classes in the living human eye. Nature 397: 520–522.

3. Roorda A, Williams DR (2002) Optical fiber properties of individual human cones. J Vis 2: 404–412.

4. Roorda A, Romero-Borja F, Donnelly W Iii, Queener H, Hebert T, et al. (2002) Adaptive optics scanning laser ophthalmoscopy. Opt Express 10: 405–412.

5. Pallikaris A, Williams DR, Hofer H (2003) The reflectance of single cones in the living human eye. Invest Ophthalmol Vis Sci 44: 4580–4592.

6. Choi SS, Doble N, Hardy JL, Jones SM, Keltner JL, Olivier SS, Werner JS (2006) In vivo imaging of the photoreceptor mosaic in retinal dystrophies and correlations with visual function. Invest Ophthalmol Vis Sci 47:2080–2092

7. Tojo N, Nakamura T, Fuchizawa C, Oiwake T, Hayashi A (2013) Adaptive optics fundus images of cone photoreceptors in the macula of patients with retinitis pigmentosa. Clin Ophthalmol 7:203–210

8. Akiyama E, Sugiyama S, Matsuzawa Y, Konishi M, Suzuki H, Nozaki T, et al. Incremental prognostic significance of peripheral endothelial dysfunction in patients with heart failure with normal left ventricular ejection fraction. J Am

Coll Cardiol.

9. Bennett AG, Rudnicka AR, Edgar DF (1994) Improvements on Littmann's method of determining the size of retinal features by fundus photography. Graefes Arch Clin Exp Ophthalmol 1994; 232:361-367. https://doi.org/10.1007/BF00175988

10. Ichiyama Y, Sawada T, Ito Y et al (2017) Optical coherence tomography angiography reveals blood flow in choroidal neovascular membrane in remission phase of neovascular age-related macular degeneration. Retina 37:724-730. https://doi.org/10.1097/IAE.0000000000001576

11. Ohtsu N (1979) A threshold selection method from gray level histograms. IEEE Trans Sys Man Cyber 9:62-66. https://doi.org/10.1109/TSMC.1979.4310076

12. Sadda SR, Guymer R, Holz FG et al (2018) Consensus definition for atrophy associated with age-related macular degeneration on OCT: Classification of atrophy report 3. Ophthalmology 125:537-548. https://doi.org/10.1016/j.ophtha.2017.09.028

13. Gune S, Abdelfattah NS, Karamat A et al (2020) Spectral-domain OCT-based prevalence and progression of macular atrophy in the HARBOR study for neovascular age-related macular degeneration. Ophthalmology 127:523-532. https://doi.org/10.1016/j.ophtha.2019.09.030

14. Duncan JL, Zhang Y, Gandhi J, Nakanishi C, Othman M, Branham KE, Swaroop A, Roorda A (2007) High-resolution imaging with adaptive optics in patients with inherited retinal degeneration. Invest Ophthalmol Vis Sci 48(7):3283–3291

15. Georgiou M, Kalitzeos A, Patterson EJ, Dubra A, Carroll J, Michaelides M (2017) Adaptive optics imaging of inherited retinal diseases. Br J Ophthalmol 15. https://doi.org/10.1136/ bjophthalmol-2017-311328.

16. Sun LW, Johnson RD, Langlo CS, Cooper RF, Razeen MM, Russillo MC, Dubra A, Connor TB Jr, Han DP, Pennesi ME, Kay CN, Weinberg DV, Stepien KE, Carroll J (2016) Assessing photo- receptor structure in retinitis pigmentosa and usher syndrome. Invest Ophthalmol Vis Sci 57(6):2428–2442. https://doi.org/10. 1167/iovs.15-18246

17. Ratnam K, Carroll J, Porco TC, Duncan JL, Roorda A (2013) Relationship between foveal cone structure and clinical measures of visual function in patients with inherited retinal degenerations. Invest Ophthalmol Vis Sci 54(8):5836–5847. https://doi.org/10. 1167/iovs.13-12557

18. Ijima H (2012) Correlation between visual sensitivity loss and years affected for

eyes with retinitis pigmentosa. Jpn J Ophthalmol 56(3): 224–229

19. Rangaswamy NV, Patel HM, Locke KG, Hood DC, Birch DG (2010) A comparison of visual field sensitivity to photoreceptor thickness in retinitis pigmentosa. Invest Ophthalmol Vis Sci 51(8):4213–4219. https://doi.org/10.1167/iovs.09-4945

20. Makiyama Y, Ooto S, Hangai M, Takayama K, Uji A, Oishi A, Ogino K, Nakagawa S, Yoshimura N (2013) Macular cone abnor- malities in retinitis pigmentosa with preserved central vision using adaptive optics scanning laser ophthalmoscopy. PLoS One 8(11): e79447 - e72013. https://doi.org/10.1371/journal.pone.0079447. eCollection

21. Cursio CA, Sloan KR, Kalina RE, Hendrickson AE (1990) Human photoreceptor topography. J Comp Neurol 292:497–523

22. Marc RE, Jones BW, Watt CB, Strettoi E (2003) Neural remodeling in retinal degeneration. Prog Retin Eye Res 22:607–655

23. Wolsley CJ, Silvestri O'NJ, Saunders KJ, Anderson RS (2009) The association between multifocal electroretinograms and OCT retinal thickness in retinitis pigmentosa patients with good visual acuity. Eye 23:1524–1531

24. Stepien KE, Han DP, Schell J et al., "Spectral-domain optical coherence tomography and adaptive optics may detect hydroxychloroquine retinal toxicity before symptomatic vision loss," Transactions of American Ophthalmological Society, vol.107, pp.28-33, 2009.

25. Debellemanière G, Flores M, Tumahai P et al., "Assessment of parafoveal cone density in patients taking hydroxychloroquine in the absence of clinically documented retinal toxicity," Acta Ophthalmologica, vol.93, no.7, pp.e534-540, 2015.

26. Jorge A, Ung C, Young LH et al., "Hydroxychloroquine retinopathy - implications of research advances for rheumatology care," Nature Reviews. Rheumatology, vol.14, no.12, pp.693-703, 2018.

27. Browning DJ, Yokogawa N, Greenberg PB et al., "Rethinking the Hydroxychloroquine Dosing and Retinopathy Screening Guidelines," American Journal of Ophthalmology, vol.219, pp.101-106, 2020.

28. Melles RB, Marmor MF., "Pericentral retinopathy and racial differences in hydroxychloroquine toxicity," Ophthalmology, vol.122, no.1, pp.110-116, 2015.

29. Ozawa H, Ueno S, Ohno-Tanaka A et al., "Ocular findings in Japanese patients with hydroxychloroquine retinopathy developing within 3 years of treatment," Japanese Journal of Ophthalmology, vol.65, no.4, pp.472-481, 2021.

30. Nohria A, Gerhard-Herman M, Creager MA, Hurley S, Mitra D, Ganz P. Role of nitric oxide in the regulation of digital pulse volume amplitude in humans. J Appl Physiol. 2006;101:545–8.

31. Hamburg NM, Vita JA. Endothelial dysfunction in atheroscle- rosis: mechanisms of impaired nitric oxide bioactivity. In: Los- calzo J, editor. Molecular mechanisms of atherosclerosis. London: Taylor and Francis; 2006. p. 95–110.

32. Hamburg NM, Keyes MJ, Larson MG, Vasan RS, Schnabel R, Pryde MM, et al. Cross-sectional relations of digital vascular function to cardiovascular risk factors in the Framingham Heart Study. Circulation. 2008;117:2467–74.

33. Widlansky ME, Gokce N, Keaney JF Jr, Vita JA. The clinical implications of endothelial dysfunction. J Am Coll Cardiol. 2003;42:1149–60.

34. Rubinshtein R, Kuvin JT, Soffler M, Lennon RJ, Lavi S, Nelson RE, et al. Assessment of endothelial function by non-invasive peripheral arterial tonometry predicts late cardiovascular adverse events. Eur Heart J. 2010;31:1142–8. doi:10.1093/eurheartj/ ehq010 (Epub 2010 Feb 24).

35. Connell PP, Keane PA, O'Neill EC, Altaie RW, Loane E, Neelam K, et al. Risk factors for age-related maculopathy. J Ophthalmol. 2009;2009:360764. doi:10.1155/2009/360764.

36. Snow KK, Seddon JM. Do age-related macular degeneration and cardiovascular disease share common antecedents? Ophthalmic Epidemiol. 1999;6:125–43.

37. Machalin´ska A, Kawa MP, Marlicz W, Machalin´ski B. Com- plement system activation and endothelial dysfunction in patients with age-related macular degeneration (AMD): possible rela- tionship between AMD and atherosclerosis. Acta Ophthalmol. 2012;90:695–703.

38. Klein R, Myers CE, Cruickshanks KJ, Gangnon RE, Danforth LG, Sivakumaran TA, et al. Markers of inflammation, oxida- tive stress, and endothelial dysfunction and the 20-year cumulative incidence of early age-related macular degeneration: the Beaver Dam Eye Study. JAMA Ophthalmol. 2014;132:446–55.

39. Machalin´ska A, Safranow K, Dziedziejko V, Mozolewska-Pio-trowska K, Paczkowska E, Klos P, et al. Different populations of circulating endothelial cells in patients with age-related macular degeneration: a novel insight into pathogenesis. Invest Ophthal- mol Vis Sci. 2011;52:93–100.

40. Kuroda Y, Yamashiro K, Miyake M, Yoshikawa M, Nakanishi H, Oishi A, et al. Factors associated with recurrence of age-related macular degeneration after anti-vascular endothelial growth fac- tor treatment: a retrospective cohort study.

Ophthalmology. 2015;122:2303–10.

41.   Mantel I, Deli A, Iglesias K, Ambresin A. Prospective study evaluating the predictability of need for retreatment with intrav- itreal ranibizumab for age-related macular degeneration. Graefes Arch Clin Exp Ophthalmol. 2013;251:697–704.

42.   Kasahara K, Moriyama M, Morohoshi K et al (2017) Six-year outcomes of intravitreal bevacizumab for choroidal neovascularization in patients with pathologic myopia. Retina 37:1055-1064. https://doi.org/10.1097/IAE.0000000000001313

43.   Kojima A, Ohno-Matsui K, Teramukai S et al (2004) Factors associated with the development of chorioretinal atrophy around choroidal neovascularization in pathologic myopia. Graefes Arch Clin Exp Ophthalmol 242:114-119. https://doi.org/10.1007/s00417-003-0803-9

44.   Muakkassa NW, Chin AT, de Carlo TE et al (2015) Characterizing the effect of anti-vascular endothelial growth factor therapy on treatment-naïve choroidal neovascularization using optical coherence tomography angiography. Retina 35:2252-2259. https://doi.org/10.1097/IAE.0000000000000836

45.   Lumbroso B, Rispoli M, Savastano MC (2015) Longitudinal optical coherence tomography-angiography study of type 2 naïve choroidal neovascularization early response after treatment. Retina 35:2242-2251. https://doi.org/10.1097/IAE.0000000000000879

46.   Cheng Y, Li Y, Huang X, Qu Y (2019) Application of optical coherence tomography angiography to assess anti-vascular endothelial growth factor therapy in myopic choroidal neovascularization. Retina 39:712-718. https://doi.org/10.1097/IAE.0000000000002005

47.   Lee JH, Lee SC, Kim SH et al (2017) Choroidal thickness and chorioretinal atrophy in myopic choroidal neovascularization with anti-vascular endothelial growth factor therapy. Retina 37:1516-1522. https://doi.org/10.1097/IAE.0000000000001384

48.   Ahn SJ, Woo SJ, Kim KE et al (2013) Association between choroidal morphology and anti-vascular endothelial growth factor treatment outcome in myopic choroidal neovascularization. Invest Ophthalmol Vis Sci 54:2115-2122. https://doi.org/10.1167/iovs.12-11542

49.   Sayanagi K, Hara C, Wakabayashi T et al (2019) Effect of intravitreal injection of aflibercept or ranibizumab on chorioretinal atrophy in myopic choroidal neovascularization. Graefes Arch Clin Exp Ophthalmol 257:749-757.

https://doi.org/10.1007/s00417-018-04214-w

50. Hata M, Oishi A, Tsujikawa A et al (2014) Efficacy of intravitreal injection of aflibercept in neovascular age-related macular degeneration with or without choroidal vascular hyperpermeability. Invest Ophthalmol Vis Sci 55:7874-7880. https://doi.org/10.1167/iovs.14-14610

51. Lois N, McBain V, Abdelkader E et al (2013) Retinal pigment epithelial atrophy in patients with exudative age-related macular degeneration undergoing anti-vascular endothelial growth factor therapy. Retina 33:13-22. https://doi.org/10.1097/IAE.0b013e3182657fff

52. Grunwald JE, Daniel E, Huang J et al (2014) Risk of geographic atrophy in the comparison of age-related macular degeneration treatments trials. Ophthalmology 121:150-161. https://doi.org/10.1016/j.ophtha.2013.08.015

53. Kuroda Y, Yamashiro K, Tsujikawa A et al (2016) Retinal pigment epithelial atrophy in neovascular age-related macular degeneration after ranibizumab treatment. Am J Ophthalmol 161:94-103.e1. https://doi.org/10.1016/j.ajo.2015.09.032

54. Cho HJ, Yoo SG, Kim HS et al (2015) Risk factors for geographic atrophy after intravitreal ranibizumab injections for retinal angiomatous proliferation. Am J Ophthalmol 159:285-292.e1. https://doi.org/10.1016/j.ajo.2014.10.035